Carrier transport properties of poly(substituted phenylacetylene)s

Shouqin Zhou, Haiping Hong, Yongxiang He, Dalin Yang, Xiangfeng Jin and Renyuan Qian*
Institute of Chemistry, Academia Sinica, Beijing 100080, China

and Toshio Masuda and Toshinobu Higashimura
Department of Polymer Chemistry, Kyoto University, Kyoto 606, Japan
(Received 9 July 1990; revised 15 February 1991; accepted 17 June 1991)

The u.v./vis. and i.r. spectra, current–voltage characteristics, carrier trapping levels and carrier mobilities of three poly(substituted phenylacetylene)s, one having an acceptor group *o*-CF_3, one having a donor group *o*-$SiMe_3$ and one having a 2,6-dimethyl-4-t-butyl group, have been studied. All three polymers show rather low conductivity, with the donor substitution leading to much higher conductivity than the acceptor substitution. Both holes and electrons take part in the severely trap-modulated conduction. In the case of poly(2,6-dimethyl-4-t-butylphenylacetylene) two trap levels with Gaussian distributions of trap energies have been found by isothermal decay current measurement. These trap energies agree closely with the apparent activation energy observed for conduction, consequently the dark conduction has its origin in thermal detrapping. In the case of poly(*o*-trimethylsilylphenylacetylene) and poly(2,6-dimethyl-4-t-butylphenylacetylene) hole and electron drift mobilities have been determined by the time-of-flight method using Scher–Montroll treatment of data to be 4×10^{-7} and 1.7×10^{-5} $cm^2 V^{-1}$, respectively, for both carriers. Donor substitution to the phenyl ring of poly(phenylacetylene) significantly enhances the photoconduction of the poly(phenylacetylene).

(Keywords: photoconductivity; poly(phenylacetylene); carrier traps; carrier mobility; volt–ampere characteristics)

INTRODUCTION

Poly(phenylacetylene) (PPA) has been of recent interest due to its photoconductivity, doping, charge transfer complex formation with acceptors and carrier transport properties[1–7]. It was found that the *trans* isomer showed slightly higher dark conductivity and much higher photoconductivity than the *cis* isomer. Acceptor doping led to enhancement of both dark and photoconductivity. From the u.v./vis. spectrum the interband transition was found to lie in the range of 300–450 nm; the limit of long wavelength tailing might depend on the extent of conjugation. Recently poly(substituted phenylacetylene)s have been synthesized, and it is interesting to study the effects of donor or acceptor substitution of the phenyl ring of PPA on the optical and electronic properties of the polymer. The optical absorption spectra, dark conductivity, carrier mobility and carrier trapping characteristics of two poly(*ortho*-substituted phenylacetylene)s, one having a donor group $SiMe_3$ and the other having an acceptor group CF_3 and one multi-donor-substituted PPA, poly(2,6-dimethyl-4-t-butylphenylacetylene), have been studied.

EXPERIMENTAL

Polymer samples. All three polymers, poly(*o*-trifluoromethylphenylacetylene) (A-PPA), poly(*o*-trimethylsilylphenylacetylene) (D-PPA) and poly(2,6-dimethyl-4-t-butyl phenylacetylene) (DD-PPA) used in this investigation were polymerized in solution with tungsten-based catalysts under the conditions listed in *Table 1*. The monomer concentration of the polymerizing solution was 1.0 M and the catalyst concentration was 10–20 mM. The polymerization time was 24 h.

Optical spectroscopy. The u.v./vis. spectra were recorded on a Shimadzu model UV190 spectrophotometer for samples in CCl_4 and on a Nanometrics model Nanospec 10 VIS-NIR microspectrophotometer for solution-cast films from $CHCl_3$. I.r. spectra of the samples as KBr compactions were recorded on a Bruker model IFS113V Fourier transform i.r. spectrometer.

Current–voltage characteristics. A polymer film (a few micrometres thick) was solution cast from a 15% w/w chloroform solution on an indium-doped tin oxide conducting glass (ITO). After the solvent was evaporated a gold electrode (12.6 mm^2) was vacuum evaporated to a thickness of 10–15 nm to form a sandwich cell for measurement.

The applied ramp voltage, positive to the ITO electrode, consisting of 20 mV steps was generated by a computer for 5 s and at this moment the current passing through the sandwich cell was measured by a Keithley model 642 electrometer. Measurements were carried out from room temperature down to −50°C in a thermostat

*To whom correspondence should be addressed

0032-3861/92/102189-05

Table 1 Polymerization conditions of the samples

Polymer	Catalyst	Solvent	Temperature (°C)	Polymer yield (%)	M_w ($\times 10^6$)	M_w/M_n
A-PPA	WCl_6-Ph_4Sn	$PhCH_3$	0	100	1.6	3.8
D-PPA	WCl_6-Ph_4Sn	$PhCH_3$	0	100	1.8	2.3
DD-PPA	$W(CO)_6$-hν	CCl_4	30	100	1.1	2.7

cooled by a semiconductor refrigerating unit and the temperature was controlled and read by two XCT-102BA1 Pt resistance thermometers. The measurement was performed automatically by a computer to obtain the current–voltage (I–V) characteristics.

Isothermal decay current measurement for trap characterization. The experimental set-up for the isothermal decay current (IDC) measurement has been described previously[6]. The sandwich cell for I–V measurement was put into a thermostatically-controlled aluminium block which can be set from 233 to 363 K. The sample was illuminated through ITO glass by an incandescent light source (58 mW cm^{-2}) while an electric field was applied to sweep the photogenerated carriers to fill the traps. When steady current was attained after 60 s, the light source was shut off and the current decay from the thermal release of trapped carriers was measured by a Keithley model 642 electrometer.

Time-of-flight mobility measurement. The sandwich cell under an applied voltage was illuminated by a 6–7 ns light pulse of $\lambda = 532$ nm from a Quanta-Ray model DCR Nd-YAG laser. The transient current passing through the cell was observed by a Hitachi model VC-6041 digital storage oscilloscope through a sampling resistor of $10^6\ \Omega$. The oscilloscope has a rise time of <8.8 ns and an input impedance of $10^6\ \Omega$ and 30 pF.

RESULTS AND DISCUSSION

Optical spectra. The u.v./vis. spectra of the samples A-PPA, D-PPA and DD-PPA in CCl_4 solution are shown in *Figure 1*; for comparison that of PPA is also shown. The conjugated backbone chain of PPA shows a not very strong absorption around 400 nm, which signifies that the conjugation length is very short – probably <10 if the absorption peak is compared with that of *trans*-polyene oligomers[8]. The absorption peaks of all three poly(substituted phenylacetylene)s show enhanced extinction coefficients with bathochromic shifts of their absorption peaks to the visible region to appear at 450, 540 and 513 nm for A-PPA, D-PPA and DD-PPA, respectively. The donor-substituted compounds shift more than the acceptor-substituted compound. It is rather difficult to interpret the bathochromic shifts as there is more extended conjugation compared to the unsubstituted PPA. One plausible reason might be the result of intramolecular charge transfer between the substituted phenyl group and the conjugated backbone chain, possibly both in the ground and in the excited states. The u.v./vis. absorption spectra (*Figure 2*) of the spin-cast films from solutions of these samples are very similar to those observed in solution but with some shift in the absorption peaks to 460, 510 and 490 nm for the A-PPA, D-PPA and DD-PPA films, respectively.

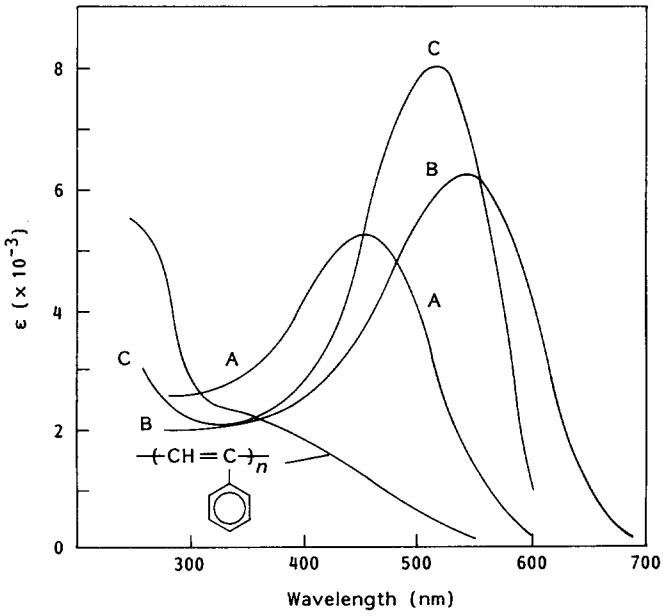

Figure 1 U.v./vis. absorption spectra of the samples in CCl_4: (A) A-PPA; (B) D-PPA; (C) DD-PPA. The absorption spectrum of PPA is also shown

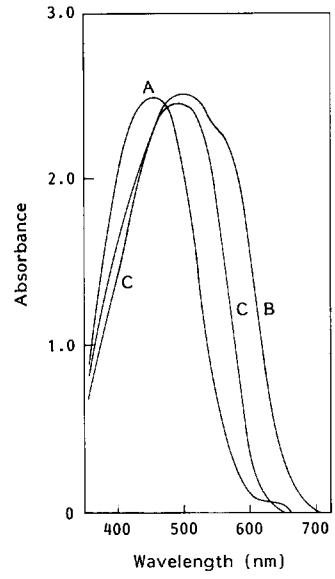

Figure 2 U.v./vis. absorption spectra of solution cast films: (A) A-PPA (0.95 μm thick); (B) D-PPA (1.48 μm thick); (C) DD-PPA (1.28 μm thick)

The i.r. spectra of these samples are shown in *Figure 3*. From the appearance of 957 and 1268 cm^{-1} bands for A-PPA, 930 and 1266 cm^{-1} bands for D-PPA and 928 and 1268 cm^{-1} bands for DD-PPA and the absorbance ratios A_{1495}/A_{1464} for A-PPA, A_{1470}/A_{1430} for D-PPA and A_{1482}/A_{1464} for DD-PPA being all greater than

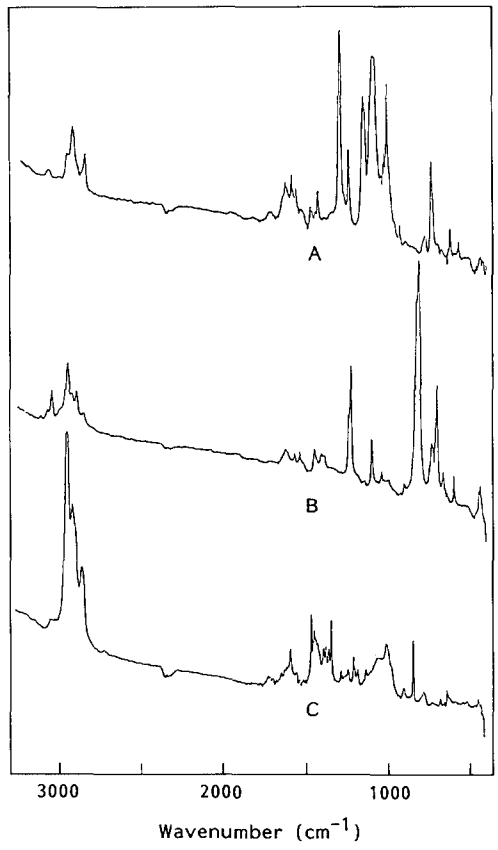

Figure 3 I.r. spectra of the samples: (A) A-PPA; (B) D-PPA; (C) DD-PPA

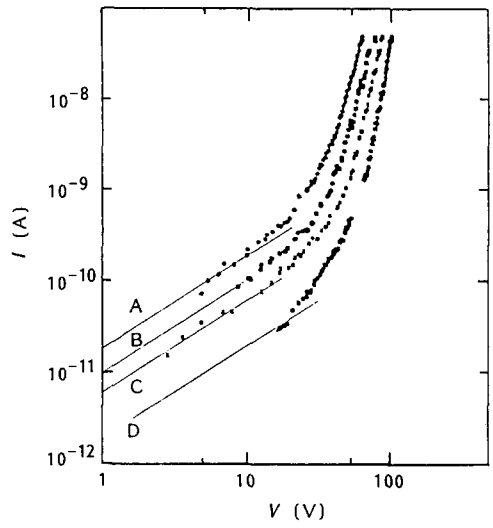

Figure 4 I–V characteristics of D-PPA (film thickness 1.95 μm). Temperature (K): (A) 300; (B) 285; (C) 275; (D) 262

unity, these poly(substituted phenylacetylene) chains are mainly of *trans* configuration[9].

Current–voltage characteristics of dark conduction. The I–V characteristics of D-PPA and DD-PPA determined at different temperatures are shown in *Figures 4* and *5*. Under low applied fields ohmic conduction was observed in both cases. This is in contrast to the recent observation of Kang *et al.*[10] of the square law dependence under such fields. Conductivity values for the samples and their energies of activation for conduction evaluated in the ohmic region are listed in *Table 2*. These apparent activation energies of conduction are much smaller than the band gap corresponding to their optical absorption peaks (~2.4 eV), so the dark conduction observed probably has its origin from thermal detrapping (see below). At high applied fields a pronounced continuous increase of the slope of the log I–log V curves up to a value of about 6 indicates a space charge limited current with a Gaussian distribution of trap energies[11].

Isothermal decay current measurement. Only the DD-PPA sample had enough photoconductivity for IDC measurement. According to the theory of Simmons[12] developed for the high field case where the released carriers have no chance to recombine, the density of states N_t and energy level E_t of the trap are given respectively by

$$N_t(E)f_0(E) = (2/eALkT)It$$

and

$$E_t = kT\ln(vt_m)$$

where I is the decay current, A is the electrode area, L is the thickness of the sample, e is the electronic charge, k is the Boltzmann constant, T is the absolute temperature, v is the pre-exponential factor for the escape of carriers from the traps, t_m is the time where the $\log(It)$ *versus* $\log t$ curve shows a maximum and f_0 is the initial (photoexcited) occupancy of the traps by the carriers and is a constant at high illumination[13]. Thus the shape of the plot $\log(It)$ *versus* $\log t$ portrays the trap energy distribution $N_t(E)$. For a Gaussian distribution of traps,

$$N_t(E) = N_0\exp[-(E - E_m)^2/\sigma^2]/(\sigma\pi^{1/2})$$

where N_0 is the total density of trapping states, σ is a distribution parameter characterizing the width of distribution and E_m is the mean trap energy where the

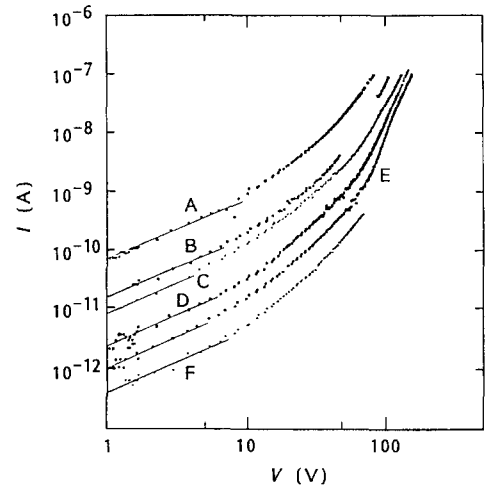

Figure 5 I–V characteristics of DD-PPA (film thickness 2.03 μm). Temperature (K): (A) 290; (B) 273; (C) 263; (D) 253; (E) 243; (F) 233

Table 2 Conductivity (σ) and activation energy (E_a) for conduction at room temperature in the ohmic region

Sample	σ (S cm^{-1})	E_a (eV)
A-PPA	8.9×10^{-16}	–
D-PPA	2.8×10^{-14}	0.30
DD-PPA	1.1×10^{-13}	0.47

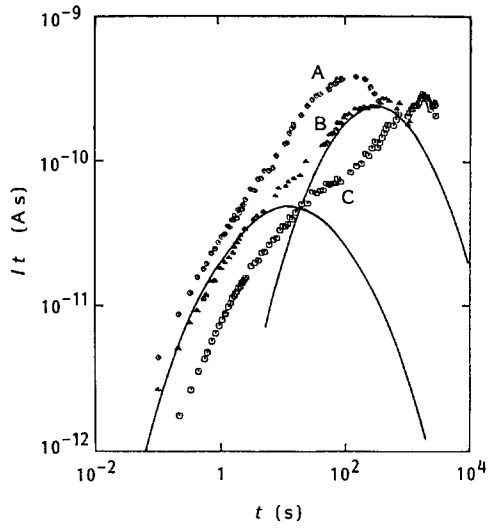

Figure 6 Isothermal decay current curves of DD-PPA film. Temperature (K): (A) 273; (B) 253; (C) 233. Applied field = 5×10^4 V cm^{-1}. Solid curves indicate fitted Gaussian distributions

Table 3 Trap parameters for DD-PPA from IDC measurement at 353 K and 5×10^4 V cm^{-1}

Trap	A	B
E_m (eV)	0.41	0.48
σ (eV)	0.045	0.032
$N_0 f_0$ (cm^{-3})	3.4×10^{19}	4.2×10^{19}
ν (s^{-1})	3.1×10^{7}	9.4×10^{7}

density of trapping states is a maximum. Simmon's theory leads to

$$\ln(It) = C_1(\ln t)^2 + C_2(\ln t) + C_3$$

where

$$C_1 = -(kT/\sigma)^2$$

$$C_2 = (2kT/\sigma^2)(E_m - kT\ln \nu)$$

$$C_3 = \ln\{[(eALkTN_0f_0)/(2\sigma\pi^{1/2})] \times \exp[-(E_m - kT\ln \nu)^2/\sigma^2]\}$$

That is

$$\sigma = kT/(-C_1)^{1/2}$$

$$N_0 f_0 = (2/eAL)(-\pi/C_1)^{1/2}\exp(C_3 - C_2^2/4C_1)$$

$$\ln \nu - E_m/kT = C_2/2C_1$$

The constants C_1, C_2 and C_3 are to be evaluated by computer fitting and then the trap parameters σ and $N_0 f_0$ are calculated. The values of E_m and ν are obtained from the plot of $C_2/2C_1$ *versus* $1/T$. The results of such measurement in the range of 233–273 K under an applied field of 5×10^4 V cm^{-1} are shown in *Figure 6*. The $\log(It)$ *versus* $\log t$ curves were fitted by two Gaussian distributions of traps, as exemplified by the curves indicated in *Figure 6* for the measurement at 253 K, to yield the trap parameters listed in *Table 3*. The two trap levels observed very probably correspond to traps for two kinds of carriers, holes and electrons. A similar result has been obtained for the case of *trans*-PPA[6]. The values of the trap energies agree very closely with the apparent activation energy for conduction observed (*Table 2*). Consequently in the DD-PPA film investigated the dark conduction is by no means intrinsic but a manifestation of thermal detrapping.

Carrier drift mobility measurement. The transient currents $I(t)$ of the sample film D-PPA (18 μm thick) for the transit of holes and electrons after a pulse illumination of highly absorbing radiation of 532 nm are shown in *Figure 7*. Severe trapping for both carriers occurred, so that no clear transit time t_T could be located directly from the transient current curve. However the transients follow the Scher–Montroll relation[14] very well. The $\log I(t)$ *versus* $\log t$ plots showed a slope of $-(1-\alpha)$ for $t \leqslant t_T$ and a slope of $-(1+\alpha)$ for $t \geqslant t_T$. The normalized Scher–Montroll plots are shown in *Figure 8*. Similar behaviour was observed for the film of DD-PPA. Carrier drift mobilities calculated from the transit times at applied fields of 2×10^5–4×10^5 V cm^{-1} are listed in *Table 4*. The holes and electrons have roughly equal mobility in both films; the values are rather small due to trap modulation. Carriers in DD-PPA

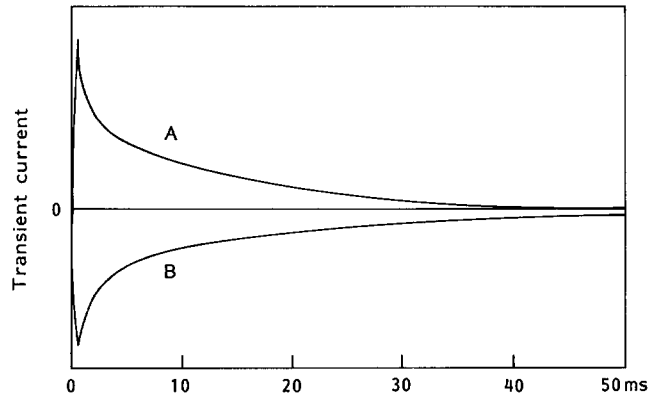

Figure 7 Transient current curves of time-of-flight measurements for holes (A) and electrons (B) in a D-PPA film (18 μm thick). Applied field = 3.75×10^5 V cm^{-1}

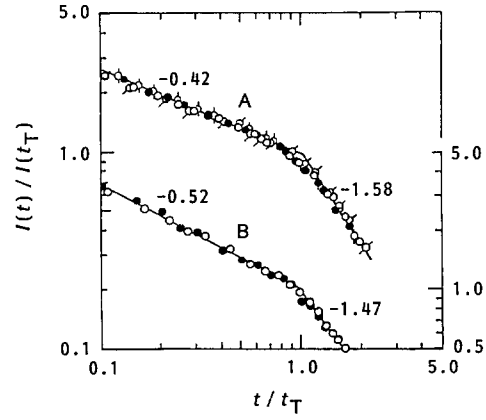

Figure 8 Scher–Montroll plots for the reduced transient current *versus* reduced time for holes (A) and electrons (B) in a D-PPA film (18 μm thick). Slopes of the straight lines before and after the transit time t_T are shown. Applied fields (V cm^{-1}): (○) 4.0×10^5; (●) $3.7_5 \times 10^5$; (◌) 3.5×10^5; (◌) 3.0×10^5

Table 4 Carrier drift mobilities of D-PPA and DD-PPA films (cm^2 V^{-1} s^{-1})

	Hole	Electron
D-PPA	4.0×10^{-7} (0.58)	4.8×10^{-7} (0.47)
DD-PPA	1.7×10^{-5} (0.40)	1.8×10^{-5} (0.30)

Numbers in parentheses are the values of the Scher–Montroll parameter α

have drift mobilities two orders of magnitude higher than those in D-PPA. Donor substitution to PPA therefore provides enhanced photoconductivity presumably through electronic interactions of the donor-substituted phenyl moiety with the conjugated electronic system of the backbone chain.

CONCLUSIONS

The substitution by donor and acceptor groups to the phenyl ring of PPA leads to enhanced electronic interaction between the phenyl π-electrons and the backbone π-conjugation. The donor-substituted PPA showed higher dark conductivity than the acceptor-substituted PPA and the multi-donor substituted DD-PPA showed the highest conductivity and highest carrier mobilities. However the carrier are severely trapped and the dark conductivities are not intrinsic but the result of thermal detrapping. Two Gaussian distributions of traps have been successfully applied to the treatment of IDC data to obtain the trap parameters. For molecular solids it is logically more natural to consider the trap distribution to be a Gaussian distribution than an exponential one, and this has been shown experimentally to be the case for PPA and substituted PPAs. The current transients of the time of flight experiments for D-PPA and DD-PPA were found to satisfy the Scher–Montroll theory very well although the photogenerated carriers were severely trapped.

ACKNOWLEDGEMENTS

This work was supported by the National Natural Science Foundation of China, Beijing National Laboratory for Structural Chemistry of Unstable and Stable Species and the United Analytical Center of Zhong Guan Cun Area, Beijing.

REFERENCES

1 Ehrlich, P. and Anderson, W. A. in 'Handbook of Conducting Polymers' (Ed. T. A. Skotheim), Vol. 1, Marcel Dekker, New York, 1986, p. 441
2 Kang, E. T., Ehrlich, P., Bhatt, A. P. and Anderson, W. A. *Macromolecules* 1984, **17**, 1020
3 Kang, E. T., Ehrlich, P. and Anderson, W. A. *Mol. Cryst. Liq. Cryst.* 1984, **106**, 305
4 Kang, E. T., Ehrlich, P., Bhatt, A. P. and Anderson, W. A. *Eur. Polym. J.* 1985, **21**, 919
5 Kang, E. T., Ehrlich, P., Bhatt, A. P. and Anderson, W. A. *Appl. Phys. Lett.* 1982, **14**, 1136
6 Jin, X., Mao, B., Zhou, S., Qian, R., Park, J. S. and Ehrlich, P. *Phys. Stat. Sol. (a)* 1989, **116**, 709
7 Hong, H., Zhou, S., Jin, X., Qian, R. and Furlani, A. *Chem. J. Polym. Sci.* 1991, **9**, 166
8 Sondheimer, F., Ben-Efraim, D. A. and Wolovsky, R. J. *J. Am. Chem. Soc.* 1961, **83**, 1675
9 Simionescu, C. I., Percec, V. and Dumitrescu, S. *J. Polym. Sci., Polym. Chem. Edn* 1977, **15**, 2497
10 Kang, E. T., Neoh, K. G., Masuda, T., Higashimura, T. and Yamamoto, M. *Polymer* 1989, **30**, 1328
11 Nespurek, S. and Smejtek, P. *Czech. J. Phys.* 1972, **B22**, 160
12 Simmons, J. G. and Tam, M. C. *Phys. Rev.* 1973, **B7**, 3706
13 Simmons, J. G. and Taylor, G. W. *Phys. Rev.* 1971, **B4**, 502
14 Scher, H. and Montroll, E. W. *Phys. Rev.* 1975, **B12**, 2455